THE ASTROPHYSICAL JOURNAL, 428:354–362, 1994 June 10

THE INFRARED TELESCOPE IN SPACE (IRTS)

H. MURAKAMI,[1] J. BOCK,[2] M. M. FREUND,[2] H. GUO,[3,4] T. HIRAO,[3] A. E. LANGE,[2] H. MATSUHARA,[3] T. MATSUMOTO,[3] S. MATSUURA,[3] T. J. MCMAHON,[5,6] M. MURAKAMI,[7] T. NAKAGAWA,[1] M. NODA,[3] K. NOGUCHI,[3] H. OKUDA,[1] K. OKUMURA,[8] T. ONAKA,[8] T. L. ROELLIG,[5] S. SATO,[3] H. SHIBAI,[1] T. TANABÉ,[9] T. WATABE,[3] T. YAGI,[10] N. YAJIMA,[1] AND M. YUI[8]

Received 1993 April 8; accepted 1993 December 10

ABSTRACT

The Infrared Telescope in Space (IRTS) is a cryogenically cooled small infrared telescope that will fly aboard the small space platform *Space Flyer Unit*. It will survey approximately 10% of the sky with a relatively wide beam during its 20 day mission. Four focal-plane instruments will make simultaneous observations of the sky at wavelengths ranging from 1 to 1000 μm. The IRTS will provide significant information on cosmology, interstellar matter, late-type stars, and interplanetary dust. This paper describes the instrumentation and mission.

Subject headings: artificial satellites, space probes — infrared: general — telescopes

1. INTRODUCTION

The Infrared Telescope in Space (IRTS) is an explorer-type instrument being developed as one of the experiments aboard the first mission of the *Space Flyer Unit* (*SFU-1*; Natori & Kuriki 1991), an unmanned, multipurpose platform facility to be launched by the Japanese HII launch vehicle and subsequently recovered by the Space Transportation System (STS) of the U.S. National Aeronautics and Space Administration (NASA). The *SFU* is a multipurpose satellite on which many experiments are loaded and operated together, sharing such satellite resources as power, telemetry, launch vehicle, and mission time. Infrared (IR) survey observations with a small-aperture cooled telescope are well matched to this type of mission. Such small telescopes can serve as very powerful tools for efficient surveys of extended sources with a relatively wide beam. The IRTS is the first Japanese orbiting telescope dedicated to IR astronomy observations.

The advantages of infrared surveys from space have been thoroughly demonstrated by missions in the past, such as the *Infrared Astronomical Satellite* (*IRAS*; Neugebauer et al. 1984) and the *Cosmic Background Explorer* (*COBE*; Mather 1982). Such missions are totally free from atmospheric absorption and emission, and cryogenic cooling of the telescope provides a very low IR background condition. In addition, recent advances in detector technology enables us to observe with even higher sensitivities than in past missions.

The IRTS employs a cryogenically cooled telescope with a 15 cm primary mirror and four focal-plane instruments which will observe the sky brightness over the 1–1000 μm wavelength region. The IRTS extends the wavelength coverage of *IRAS* to both shorter and longer wavelengths with higher sensitivity. In addition, the IRTS will add additional spectral information to the results of *COBE* in the near-to-far-IR region, where important spectral features such as the near-to-mid-IR unidentified band emissions and far-IR [C II] and [O I] lines are found. The IRTS will also observe the submillimeter sky brightness with a higher spatial resolution than the *COBE* mission. The following sections give an overview of the hardware of the IRTS and an outline of the IRTS mission, including the scientific goals.

2. MISSION DESCRIPTION

2.1. *SFU-1 and IRTS Mission*

The *SFU* is a space-platform facility designed around an octagonal truss structure with a diameter of approximately 4.5 m (Fig. 1). Eight thermally controlled payload boxes, two for the core system and six for the user experiments, are attached to the truss. The user instruments can also be accommodated on the exposed upper deck and in the center hole. The core system of the *SFU* provides the electrical power, telemetry link, and attitude and orbit control to the user experiments. *SFU* system performance is summarized in Table 1. The *SFU* was developed by three Japanese organizations: the Institute of Space and Astronautical Science (ISAS), the National Space Development Agency (NASDA), and the Institute for Unmanned Space Experiment Free Flyer (USEF).

In the configuration used in the *SFU-1*, the orbit change thruster is mounted in the center hole, and the IRTS is directly attached to the *SFU* truss, replacing one of the payload boxes.

The IRTS is a cryogenically cooled telescope. The telescope system and the focal-plane instruments (FPIs) are contained in a cryostat 93 cm in diameter and 110 cm long (Fig. 2). The aperture cover of the telescope, which is a part of the vacuum shell of the cryostat while on the ground, will be ejected in orbit. A circular aperture shade used for rejection of IR radiation from the Earth and three electronics boxes are attached

[1] Institute of Space and Astronautical Science, Yoshinodai 3-1-1, Sagamihara, Kanagawa 229, Japan.
[2] Department of Physics, University of California, Berkeley, CA 94720.
[3] Department of Astrophysics, School of Science, Nagoya University, Furocho, Chikusa, Nagoya 464, Japan.
[4] Present address: Beijing Observatory, Beijing 100080, China.
[5] Space Science Division, NASA Ames Research Center, Moffett Field, CA 94035-1000.
[6] Present address: Yerkes Observatory, P.O. Box 258, Williams Bay, WI 53191.
[7] Institute of Engineering Mechanics, University of Tsukuba, Tsukuba, Ibaragi 305, Japan.
[8] Department of Astronomy, Faculty of Science, University of Tokyo, Bunkyo-ku, Tokyo 113, Japan.
[9] Institute of Astronomy, Faculty of Science, University of Tokyo, Mitaka, Tokyo 181, Japan.
[10] Department of Mechanical System Engineering, Tokyo Metropolitan Institute of Technology, Hino, Tokyo 191, Japan. Present address: Nippon Denso, Kariya, Aichi 448, Japan.

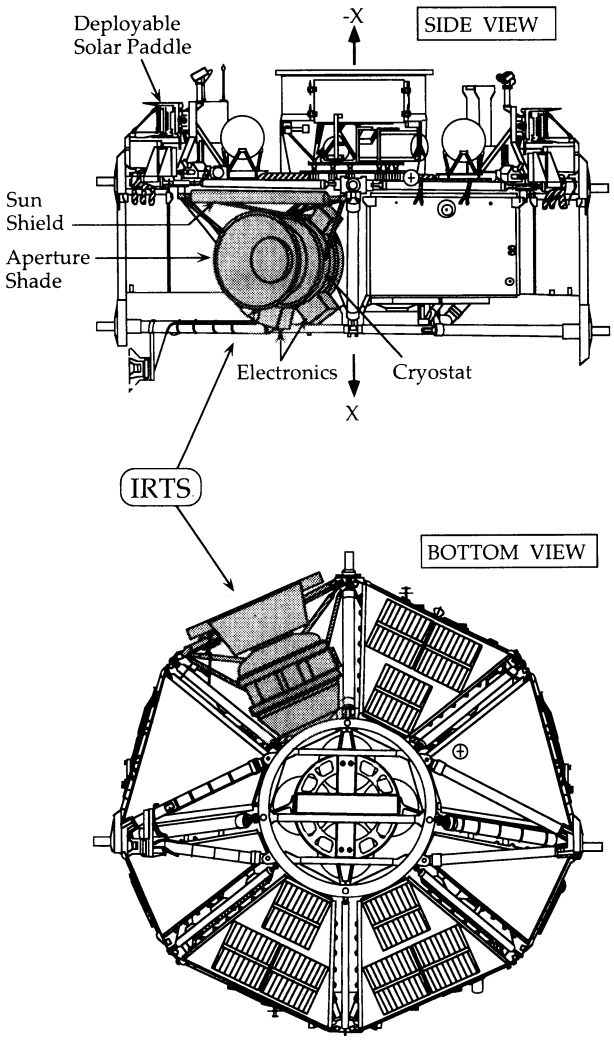

FIG. 1.—Side view and top view of the *SFU-1*. The IRTS is shaded.

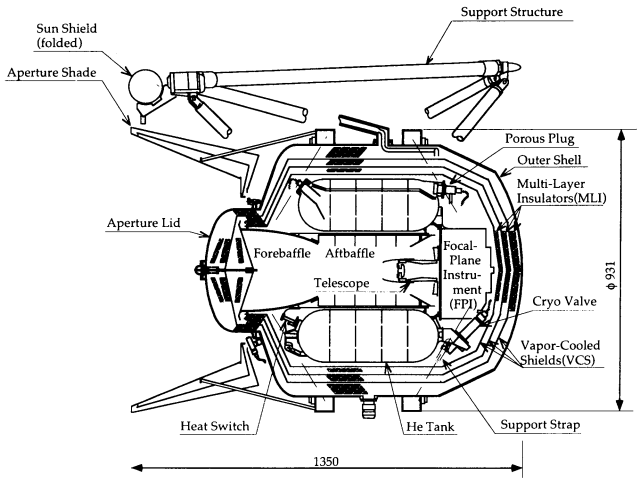

FIG. 2.—Cross-sectional view of the IRTS. Typical dimensions are indicated in millimeters.

to the outer shell of the cryostat. The whole system of the IRTS is attached to the *SFU* truss through a support structure. A deployable sun shield is fixed on this support structure.

Other *SFU-1* experiments, including experiments in material science, life science, and some technology demonstrations, are accommodated in the remaining five payload boxes and on the upper deck. The launch weight of the complete *SFU-1* is approximately 4×10^3 kg.

The *SFU-1* is scheduled to be launched in February 1995 by an HII launch vehicle under development by the NASDA. The *SFU-1* will initially be injected into a low Earth orbit. Thirty minutes after launch, the IRTS electrical power will be turned on and the dedicated experiment processor (DEP) will automatically open the helium vent valve. The *SFU-1* system will spend the first several days in orbit checking the core system. During this period, the *SFU* will move up to the experiment operation orbit, a circular orbit of approximately 500 km altitude and 28°.5 inclination. This time will also be used in degassing the satellite surfaces.

The IRTS experiment will commence by deploying the sun shield and ejecting the aperture lid. The IRTS observations will last for 20 days. During this observation period, the IRTS will survey approximately 10% of the entire sky and will make absolute measurements in the near-to-mid-IR and submillimeter regions. In addition, the IRTS will also survey far-IR fine-structure line intensities of carbon ions and oxygen atoms.

The down links of the IRTS telemetry data will be supported by the Kagoshima Space Center of the ISAS and by three receiving stations of NASA's Deep Space Network (DSN), located at Goldstone, Canberra, and Madrid. In about two-

TABLE 1

PERFORMANCE OF THE *SFU* (NATORI & KURIKI 1991)

Item	Performance
Weight	Approximately 4.0×10^3 kg at launch
Dimensions	4.46 m diameter × 2.8 m
Electric power	1.4 kW (3 kW paddle-generated power)
Command and data Management system	S-band link Telemetry: 128 kbits s^{-1} Command: 1 kbits s^{-1} Data recorder: 80 Mbits Data rate: 16 kbits s^{-1} maximum
Navigation and guidance control	Navigation: Global Positioning System and Inertial Reference Unit Guidance: onboard software Control: 3 axis stabilized, 1° accuracy
Reaction control system	Hydrazine monopropellant system
Experimental resources	Six payload units (PLUs), 150 kg per unit Upper deck and center hole μG level: $>10^{-4}$ G Available power for experiments: 1 kW

thirds of the observational orbits, the IRTS will be visible from these stations at least once per orbit and will generate data at the rate of 6 kbits s^{-1}. For those orbits where the IRTS will not pass over a ground station, the IRTS data rate will be reduced to 3 kbits s^{-1}. The data acquired by the Kagoshima Space Center will be transferred to the Sagamihara Operations Center (SOC) of ISAS in real time, and those acquired by the DSN stations will be transferred to the SOC through the Jet Propulsion Laboratory with a 1 hr delay. The data will then be distributed to each experiment monitoring system.

After the IRTS observation period, the sun shield will be ejected to allow for recovery by NASA's STS system. The *SFU* will descend to the retrieval orbit of 315 km altitude at the end of its 6 month mission and will then be retrieved by the Space Shuttle.

2.2. *Attitude Control and Sky Survey*

The IRTS itself has no pointing capability. The scan paths in the sky are determined by maneuvering the entire *SFU* system. The *SFU-1* will be operated in the solar-oriented attitude where the $-x$-axis of the *SFU-1* (see Fig. 1) is pointed toward the Sun. During the IRTS observations, the *SFU* is rotated around this $-x$-axis once per orbital revolution at a constant rate. Because the optical axis of the IRTS is perpendicular to the $-x$-axis, this attitude results in the IRTS scanning the sky along great circles at right angles to the Sun (Fig. 3). The sky observed by the IRTS will change at a rate of approximately 1° per day with the orbital motion of the Earth around the Sun.

The IRTS rotation direction and phase will be determined so as to maximize the angular distance from the IRTS optical axis to the Earth limb. There are basically two scanning modes. At the center of the day side on the orbit, the IRTS is directed to the north when the *SFU* passes through the northern side of the subsolar point (mode 1), or directed to the south when the *SFU* passes through the southern side (mode 2). Figure 3 shows the *SFU* attitude in mode 1. Rotation in mode 2 is in the opposite direction. As shown in Figure 3, the $-x$-axis is in fact slightly off of the Sun line (angle g in the figure), southward or northward depending the scanning mode, to avoid IR radiation from the Earth limb, which is only 22° below the horizontal direction on the spacecraft.

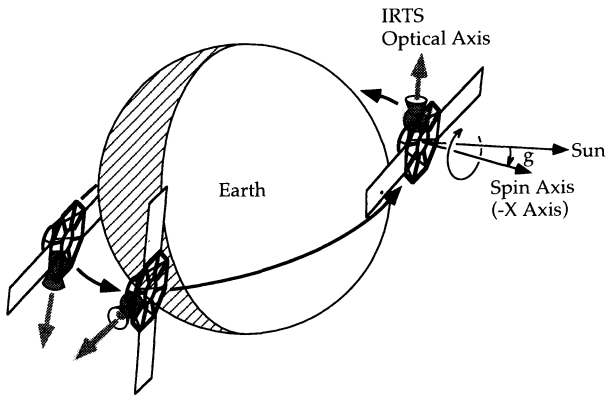

FIG. 3.—Attitude control of the IRTS in the mode 1 is illustrated

The required attitude control depends on the date and time of launch and on when the IRTS will begin its observations. Therefore, the final attitude control sequence, including the selection of the mode mentioned above and detailed optimization, will be determined once the *SFU-1* is launched. Figure 4 shows an example of the observed sky area. This figure assumes that the *SFU* will be launched at UT 9^h20^m on 1995 February 15 and that the IRTS will start observations on

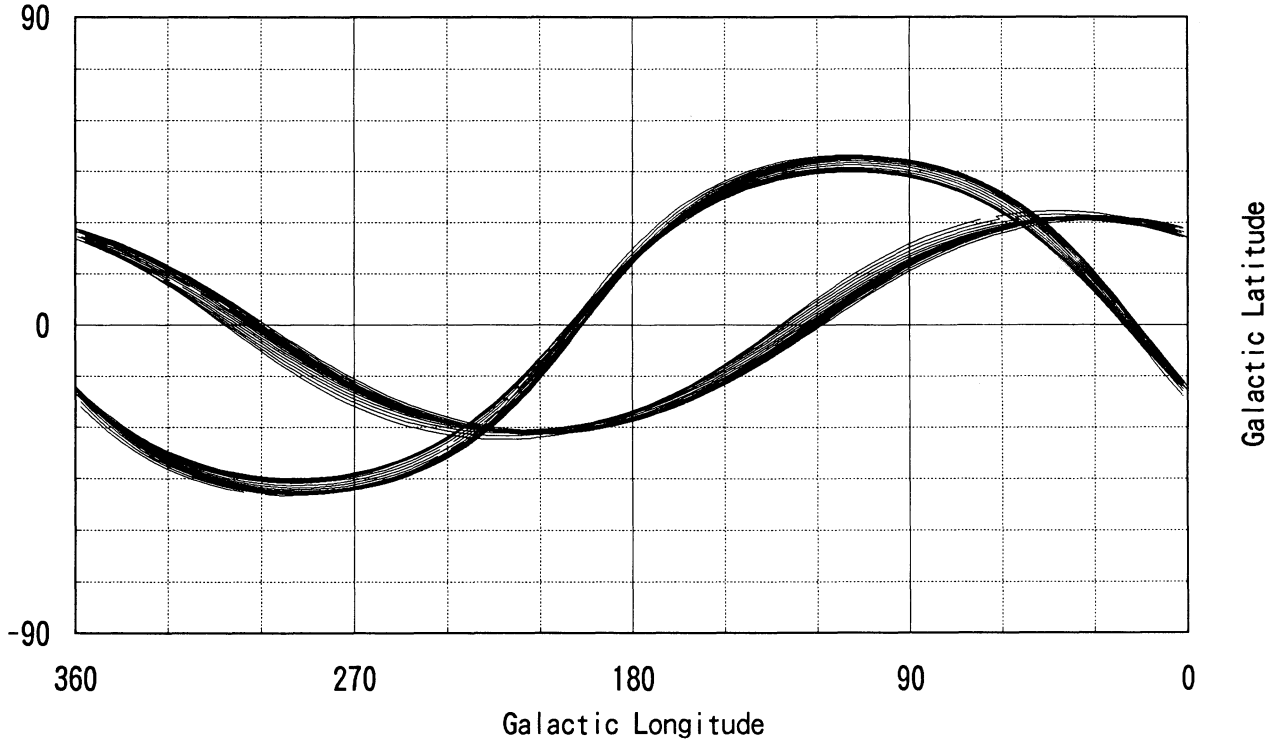

FIG. 4.—Example of the observed sky area is shown in galactic coordinates. A launch at UT 9^h20^m on February 15 is assumed. The scan mode is changed from mode 1 to mode 2 in the middle of the observation period, and the two bands in the figure correspond to the observing areas before and after the mode change.

the eighth day after launch. In addition, the attitude control mode is assumed to change from mode 1 to mode 2 on the 17th day after launch.

The accuracy of the *SFU* attitude-control system is $\sim 1°$. The actual scan path will be reconstructed to an accuracy of 1 arcmin after the mission, using the data from the gyroscopes of the *SFU* core system and the IRTS star sensor, which is located on the IRTS telescope focal plane together with the FPIs.

3. IRTS MISSION HARDWARE

3.1. *Cryostat*

A cross-sectional view of the IRTS cryostat is given in Figure 2. A complete description of the IRTS cryostat is given in Murakami et al. (1990). The cryostat has a torus-shaped liquid helium tank with a volume of 100 liters. This tank will be filled to 90% full with superfluid helium by two successive transfers shortly before launch. In the first transfer, the tank will be filled with normal helium and then pumped to convert the helium to a superfluid state. In the second transfer, the tank will be filled with helium at a temperature slightly higher than the lambda point and again pumped. The pumping will last until 11 hr before launch, in the present operation schedule. The helium tank will be closed during the ascent of the vehicle and then opened to outer space to continue the evacuation.

The telescope and the FPIs are attached to the bottom of the helium tank and operate at a temperature of 1.9 K. The helium tank is suspended from the outer vacuum shell by 12 support straps which are made of glass fiber–reinforced plastic. Three vapor-cooled shields (VCS) to shield the helium tank from IR radiation are also supported by these straps.

A porous plug made of alumina ceramics is employed as a phase separator, separating the vapor from the liquid helium in zero gravity. Helium gas evaporated through the porous plug first cools the forebaffle and then circulates through the VCSs.

The aperture lid has two radiation shields. These shields are passively cooled by thermal contact with the outer VCS and the forebaffle. The aperture lid will be ejected by springs at the beginning of the IRTS observational period.

The thermal performance of the cryostat has been evaluated by numerical model calculation and confirmed by testing. The temperature distribution results are compiled in Table 2. The heat load to the helium tank is about 70 mW, half of which is due to heat conduction through the support straps. The FPIs generate about 10 mW. The expected hold time of the liquid helium is greater than 35 days after launch, under standard conditions.

3.2. *Telescope and Baffling System*

The IRTS telescope is a Richey-Chretien system with a effective diameter of 15 cm and a focal length of 600 mm, F/4 (Onaka et al. 1994). The mirrors are made of aluminum alloy, cut by a high-precision numerically controlled machine, and coated with Ni before final cutting and polishing. The surface of the mirrors are coated with 0.2 μm Au and 0.1 μm SiO_2.

The primary mirror cell and the secondary mirror support are also made of aluminum alloy to minimize the degradation of image quality due to differential thermal contraction. A schematic view of the telescope system together with the FPIs is given in Figure 5. The secondary mirror is supported by four stays from the central hole of the primary mirror. This configuration prevents the supporting stays from being directly illuminated by stray light scattered from the forebaffle.

TABLE 2

TEMPERATURE DISTRIBUTION OF THE CRYOSTAT IN ORBIT

Position	Expected Best Case[a]	Worst Case[b]
Conditions		
Outer shell[c]	300 K	300 K
Aperture heat load[d]	10 mW	200 mW
Heat switch[e]	ON	OFF
Temperatures (K)		
Outer VCS	201.3	191.6
Middle VCS	107.5	96.5
Inner VCS	24.3	26.1
Forebaffle	2.6	18.7
He Tank	1.9	1.9

[a] The requirements of Sun and Earth avoidance are both satisfied.

[b] Radiation from the earth directly illuminates the upper part of the forebaffle. The heat switch is turned off to reduce the heat load to the helium tank.

[c] The accurate calculation of the outer shell temperature is very difficult, because of the complex structure of the *SFU*. A temperature of 300 K is assumed here for both cases.

[d] Heat absorbed by the forebaffle.

[e] Heat switch for the forebaffle (see text).

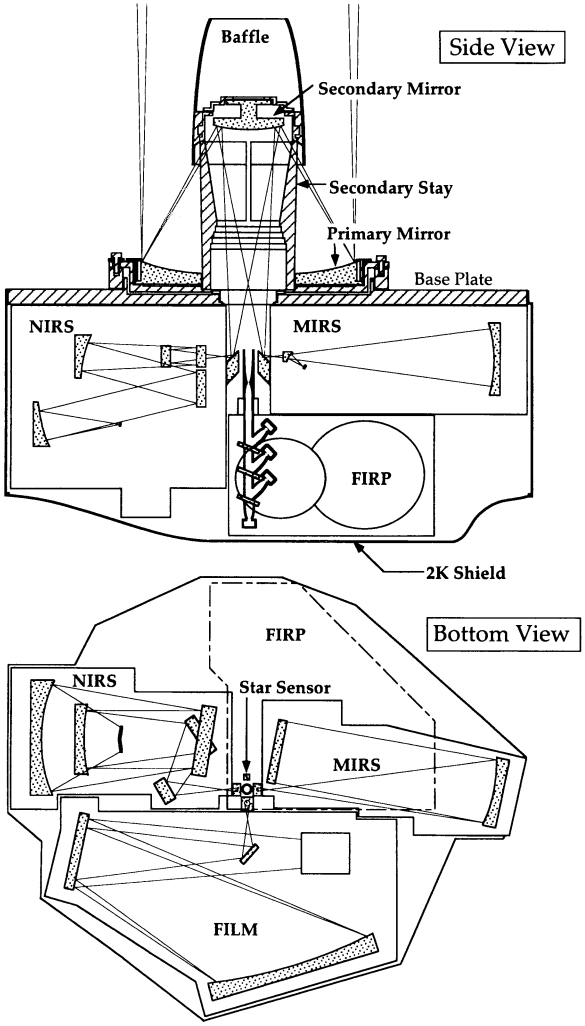

FIG. 5.—Arrangement of the telescope system and the FPIs

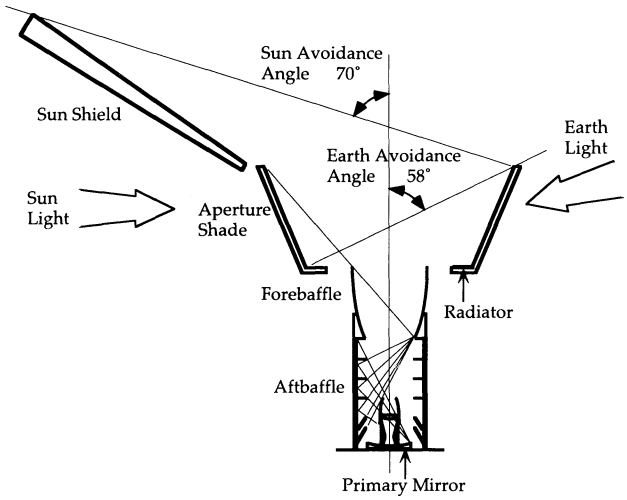

FIG. 6.—IRTS baffle system

Because the IRTS is intended to make absolute measurements, good sidelobe rejection is required for the baffling system. Figure 6 shows the concept of the baffle system (Sato et al. 1994). The sun shield is a carbon fiber–reinforced plastic sheet, 2 m long, covered with an aluminized Teflon film on the surface that is illuminated by sunlight. On the ground, the sun shield is stowed rolled up and, in orbit, is deployed to block the direct incidence of sunlight into the aperture shade. The aperture shade has a specular inner surface that reflects thermal radiation from the Earth and the sun shield. It has two layers of radiation shielding and is cooled to below 200 K by a radiator located at the bottom. The forebaffle is a Winston-type reflector (Winston 1970) made of aluminum alloy coated with Au and reflects the thermal radiation of the aperture shade back to the sky. This reflecting forebaffle is essential for the cryostat design, since it reduces the aperture heat load considerably and makes the cryogenic system more compact. The forebaffle is usually cooled by evaporated helium to about 10 K. It can be cooled to below 4 K, depending on the observation mode in use, by a thermal connection to the helium tank through a heat switch, making the thermal emission negligible even in the submillimeter region. The heat switch utilizes copper cylinders separated by a small gap which is filled or emptied of helium gas to achieve the switching action (Duband, Hui, & Lange 1990). The last stage of the baffle system is the aftbaffle, which consists of a set of annular vanes. The aftbaffle is coated with a special paint chosen for its mechanical strength and its nearly perfect black properties from the near-IR to millimeter wavelengths (Bock & Lange 1994).

The combined performance of the forebaffle and the aftbaffle was evaluated at visible wavelengths in the laboratory and a high submillimeter sidelobe rejection was confirmed by a rocket experiment at 90 μm and 180 μm (Bock et al. 1994).

3.3. *FPIs*

Four scientific instruments, the Near Infrared Spectrometer (NIRS), the Mid Infrared Spectrometer (MIRS), the Far Infrared Line Mapper (FILM), and the Far Infrared Photometer (FIRP) are installed in the focal plane of the telescope together with a near-IR star sensor.

The NIRS is a spectrometer with a fixed grating and linear InSb arrays (Noda et al. 1994). It covers the shortest wavelengths of the IRTS coverage, 1.4–4.0 μm, with moderate resolution, $\Delta\lambda = 0.12$ μm. The detectors consist of two 12-element InSb photodiode arrays aligned in the dispersion direction. Twenty-four channel charge integrating amplifiers, which are constructed with junction field effect transistors (JFETs), are operated at about 70 K with a readout noise of approximately 150 electrons.

The MIRS is a very simple and lightweight spectrometer covering the 4.5–11.7 μm wavelength range (Roellig et al. 1994). The light passing through the entrance slit is dispersed and refocused by a concave grating onto 32 off-axis parabolic field mirrors, which then focus the dispersed image onto 32 Si:Bi photoconductive detectors. The newly developed grating has variable line spacings and blaze angles. This grating realizes an astigmatism-free image and a flat focal plane at a given wavelength. The spectral resolution ranges from a minimum of 0.23 μm at a wavelength of 6.7 μm to 0.36 μm at 10.8 μm.

The FILM is also a grating spectrometer. This instrument has the highest spectral resolution, $\lambda/\Delta\lambda = 400$, among the four FPIs and is designed to observe the fine-structure lines emitted by carbon ions and oxygen atoms (Shibai et al. 1994). A grating design similar to that employed in the MIRS was also adopted for the FILM. The FILM grating has a cylindrically concave shape and gradually varying line spacings. The [C II] and the [O I] lines are detected by stressed and nonstressed Ge:Ga photoconductive detectors, respectively. The FILM also has continuum channels at 155 μm and 160 μm, one on either side of the [C II] line wavelength.

The FIRP is a four-channel photometer covering the submillimeter wavelength region (Lange et al. 1994). Filters and dichroic beam splitters separate the incident light into four wavelength bands. The center wavelengths are approximately 140 μm, 230 μm, 400 μm, and 700 μm. Each channel has a matched pair of composite bolometers, one illuminated by incident light and the other in a dark cavity. Each pair is biased in an AC bridge. Lock-in amplifiers detect only the difference of signals from paired bolometers, producing a stable output signal proportional to absolute power (Wilbanks et al. 1990). The bolometers are cooled to 300 mK by a closed-cycle ^{3}He refrigerator (Duband et al. 1990).

A Ge photodiode with a slant mask is placed at the focal plane as a star sensor. The wavelength band, which is determined by the spectral response of the Ge photodiode operated at 2 K itself, is similar to the standard IR J-band. The Ge photodiode has a 17^2 arcmin^2 field of view and will detect stars brighter than $m_J = 6$ mag (5 σ). Using this star sensor, the data from the gyroscopes can be calibrated once every few minutes with an accuracy of 0.″02.

All FPIs except the star sensor, have cold shutters, which are periodically closed during the observation in order to calibrate zero signal levels. These instruments also have internal light sources of proper color temperatures which allow the detector responsivities to be periodically measured in flight.

Figure 5 shows the arrangement of the instruments on the focal plane. The NIRS, MIRS, and FILM have ~45° mirrors in front of the entrance slits and pick off beams 1° off the optical axis. The FIRP uses the on-axis beam to achieve the best sidelobe rejection of the baffling system. The star sensor is also located at 1° off the optical axis. All of the FPIs are surrounded by a shield cooled to a temperature of approximately 2 K to reject the far-IR emission from the VCSs. The 2 K shield was made of thin aluminum plates and aluminum foil lined with Kapton film.

The FPI system with the flight telescope was tested in the laboratory using a special test cryostat prior to its installation into the flight cryostat. The test cryostat had a vacuum window and a neutral-density filter system to introduce an IR beam from external light sources at backgrounds similar to those expected in orbit. The beam pattern and responsivity of each FPI was evaluated in this configuration, except for the FIRP responsivity, which was measured with a low-temperature blackbody source inside the test cryostat.

The FPI system was then installed into the flight cryostat, and its performance was checked in a dark condition with a cold cover over the telescope forebaffle. In this test, no measurable light leak was detected by any instrument, a very important result for absolute measurements. We found an unknown light source inside the FILM, but it did not affect the zero signal levels of FPIs other than the FILM. Noise performance, including the effects of electrical interference among the FPIs and the other electronic components, was then evaluated. The noise floor due to electrical interference and cold preamplifier noise contributed equally to the noise performance of the NIRS and the MIRS. However, the sensitivity of the MIRS will be limited by the Poisson noise of the relatively strong zodiacal background in all but the very shortest wavelength channels. Noise due to the unknown internal light source and to electrical interference dominates for the FILM. The major noise source for the FIRP and the star sensor is electrical interference.

Figure 7 shows the measured FPI beam sizes (FWHM) and the relative beam positions projected on the sky. The beams of the NIRS and the MIRS are aligned in the scan direction, and they will observe approximately the same sky region with a time delay of about 30 s.

The 1 σ sensitivity of each instrument per field of view calculated from the measured laboratory performance is shown in Figure 8, with the brightness of some known extended sources. The integration time is approximately 64 s for FIRP, 6 s for FILM, and 4 s for MIRS and NIRS. The IRTS sensitivity is compared with the sensitivity for *IRAS* (Neugebauer 1984) and for the DIRBE and the FIRAS instruments on the *COBE* mission (Hauser et al. 1991). The NIRS and the MIRS are less sensitive than the DIRBE instrument, but they have a higher angular and spectral resolution with nearly continuous coverage over 1.4–12 μm. The FILM has spectral resolution similar to that of the FIRAS instrument near 100 μm, but has much higher sensitivity and angular resolution. The FIRP has angular resolution similar to that of the DIRBE, but has much higher sensitivity. A summary of the characteristics of the four FPIs is given in Table 3.

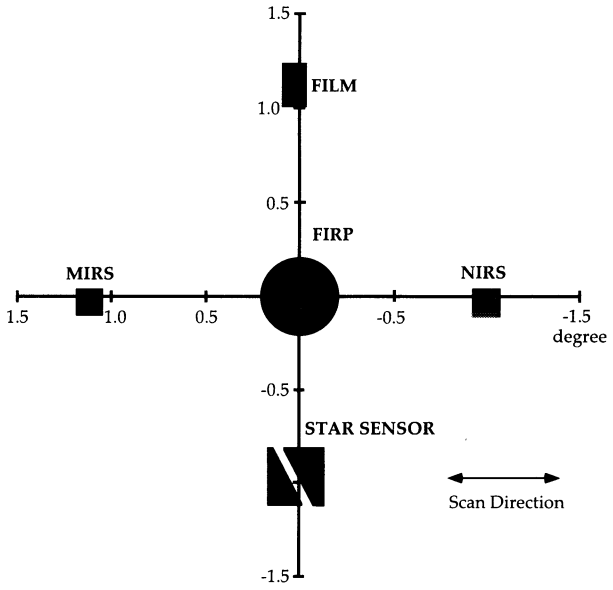

FIG. 7.—FPI field of view. Each shaded figure shows the relative position of the beam and the FWHM beam size. The shapes are rendered schematically only.

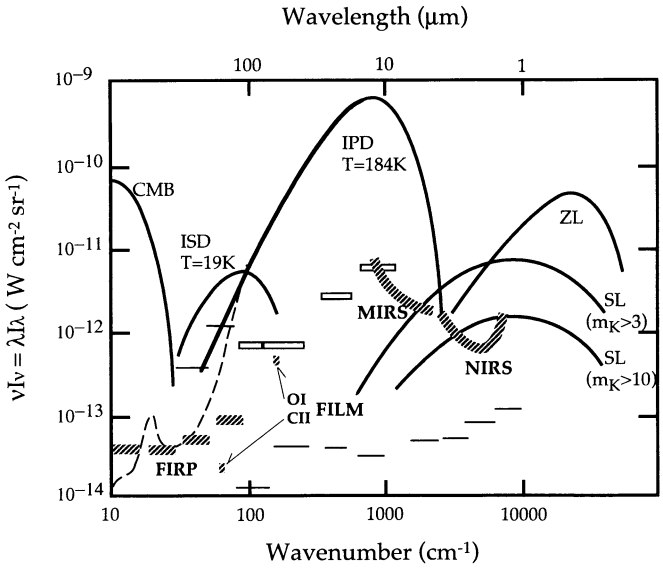

FIG. 8.—Detection limits of the FPIs are indicated by hatched patterns. For the FILM, line intensities detectable with 1 σ are plotted. The detection limits are 1 σ per field of view, based on the measured laboratory performance of the fully integrated system. Solid lines show components of sky brightness: zodiacal light (ZL), thermal emission of the interplanetary dust (IPD), integrated star light (SL), thermal emission of the interstellar dust (ISD), and 2.74 K cosmic background radiation (CMB). For the integrated starlight, the contributions from stars fainter than 3 mag at K band and from only stars fainter than 10 mag are shown. The 1 σ sensitivity of the *COBE*/DIRBE experiment (*horizontal bars*), the *COBE*/FIRAS experiment (*dashed line*) for a 1 year mission (from Fig. 3 of Hauser et al. 1991), and the *IRAS* survey (*open rectangles*; Neugebauer et al. 1984) are also shown.

3.4. *The Electronics and Telemetry Data System*

The electronics system of the IRTS consists of three parts, a dedicated experiment processor (DEP), a data processing unit (DPU), and the FPI electronics (FPI-E). The FPI-E amplify the signals from the four FPIs and the Ge star sensor and converts them to digital data of 16 bit length. In addition, this electronics package adjusts the bias voltages of the IR sensors and drives the cold shutters and internal calibration sources according to the commands. The DPU processes the housekeeping signals, which come mainly from thermometers in the cryostat. For housekeeping data, the word length is 8 bits.

Each experiment onboard the *SFU-1* has its own microprocessor, and this processor controls the sequence of the experiment. The control of the IRTS observational sequence, however, is very simple because the observation is a uniform sky survey. The IRTS DEP only generates the command sequences for an automatic in-flight calibration of the FPIs. The most important of these sequences are the commands for opening/closing the FPI shutter and turning the calibration

TABLE 3

FPI CHARACTERISTICS

ITEM	FPI			
	NIRS	MIRS	FILM	FIRP
Optical system	Grating spectrometer	Grating spectrometer	Grating spectrometer	Wide-band photometer
Wavelength coverage	1.4–4.0 μm	4.5–11.7 μm	63 μm ([O I]) 158 μm ([C II]) 155, 160 μm (continuum)	140, 230, 400, 700 μm
Wavelength resolution	$\Delta\lambda = 0.12$ μm	$\Delta\lambda = 0.23$–0.36 μm	$\lambda/\Delta\lambda = 400$ for [O I] and [C II] $\lambda/\Delta\lambda = 150$ for continuum	$\lambda/\Delta\lambda = 3$
Beam size	8′ × 8′	8′ × 8′	8′ × 13′	30′ circle
Detector system	Two InSb 12-element arrays	Si:Bi × 32	Ge:Ga × 1 Stressed Ge:Ga × 3	0.3 K bolometer × 4
	Charge integrating amplifiers	Charge integrating amplifiers	Transimpedance amplifiers	AC-biased bridge circuit

source on/off, which are used to check sensitivity changes and zero-level drifts of the FPI signal output. This calibration sequence will be done every 17.5 minutes during the IRTS observation period.

The most important job of the DEP is to handle the telemetry data. The DEP gathers the data of the FPIs and the housekeeping system following a given telemetry format and passes them to the Command and Data Management System (CDMS) of the *SFU*. The IRTS has three telemetry modes. Telemetry format 1 is designed for a normal observational mode, in which the IRTS generates data at the rate of 6 kbits s^{-1} and the data are sent to the ground once every orbital revolution. The FPI data occupies 94% of the 6 kbits s^{-1}, and the housekeeping data and other engineering data the remaining 6%. In orbits where the IRTS does not pass over a receiving station, the data rate is limited by the capacity of the onboard data recorder. During these orbits, the DEP reduces the data rate to one-half of the normal mode, 3 kbits s^{-1} (telemetry format 2), by halving the sampling rate of all the data except for the NIRS. Only data from odd-numbered detectors of the NIRS are sampled in this telemetry mode. The last mode is a standby mode in which only housekeeping data are sent to the ground, with a very low data rate, about 24 bits s^{-1}. The telemetry mode change is performed by commands from the ground. Those commands, as well as other control commands of the IRTS, are first stored in the main computer of the *SFU-1* and subsequently passed to the IRTS DEP at a given time, to be executed.

Opening the aperture-lid and deploying/jettisoning the sunshield are performed using pyro-devices, which are directly controlled by the core system of the *SFU-1*. The characteristics of the IRTS hardware are summarized in Table 4.

4. SCIENTIFIC GOALS

4.1. *Interplanetary Dust*

The *IRAS* mission observed the thermal emission from interplanetary dust in the mid-to-far-IR range at solar elongation angles near 90° (Hauser et al. 1984). However, the *IRAS* could not take spectra of this observed dust emission. Also, information on sunlight scattered by the planetary dust is still poor in the IR region compared with that from optical and UV wavelengths.

The size distribution and the composition of the interplanetary dust will affect the IR spectra of both the scattered light and the thermal emission. The nearly continuous spectra obtained by the NIRS and the MIRS in the wavelength range 1.4–11.7 μm, which includes the silicate feature at 9.7 μm, is an ideal tool for investigating interplanetary dust.

TABLE 4

CHARACTERISTICS OF THE IRTS

Item	Characteristics
Weight	Total weight: 183 kg Cryostat: 128 kg FPI + telescope: 9 kg Electronics: 16 kg Support structure: 18 kg Others: 12 kg
Dimensions	93 cm diameter (cryostat) × 135 cm (including aperture shade)
Power consumption	80 W maximum
Cryostat	Superfluid helium, 90 liters FPI temperature: 1.9 K Cold lifetime: >35 days after launch
Telescope	15 cm diameter F/4 Ritchey-Chretien type Effective collecting area: 113 cm^2
FPIs	Near-Infrared Spectrometer (NIRS) Mid-Infrared Spectrometer (MIRS) Far-Infrared Line Mapper (FILM) Far-Infrared Photometer (FIRP)
Telemetry	Data rate: 6 kbits s^{-1} (visible orbit), 3 kbits s^{-1} (invisible orbit)
Observation	20 days, uniform sky survey
Sky coverage	Approximately 10% of the entire sky

4.2. *Interstellar Matter*

The observation of interstellar matter is one of the major goals of the IRTS mission. The FIRP's sensitivity, spectral coverage, and angular resolution enable it to study emission from cold interstellar dust particles, which constitute most of the dust mass. These measurements will yield basic knowledge about the total mass of the dust clouds.

A *COBE* experiment has found evidence for a low frequency (<30 cm^{-1}) excess in the submillimeter spectra of the interstellar dust, that may be due to very cold (4.77 K; Wright et al. 1991) dust. The FIRP covers the entire spectral range from 100 μm to 1 mm and, thus, covers the region where emission from the cold dust component should be observable. The FIRP will determine whether this cold component is morphologically distinct from the warm ($\sim$20 K) component on angular scales of 0°.5.

The spectra of the diffuse clouds have a hot component which is bright in the mid-IR region as well (Boulanger, Baud, & Albada 1985). This component is postulated to be due to very small dust particles transiently heated by a single UV photon. These very small particles are also believed to be the origin of the IR band emissions located at 3.3, 3.4, 6.2, 7.7, 8.6, and 11.3 μm. The NIRS and the MIRS have the sensitivity to detect even weak features from the clouds illuminated by the general interstellar UV field without nearby sources. These two instruments will study the spatial variation of these features within the galaxy.

The UV photons which hit the dust particles also dissociate molecules and heat up the gas in the clouds through a photoelectric heating process. The FILM will trace the resulting warm gas by observing the [C II] and the [O I] lines. The [C II] line at $\lambda = 158$ μm is the most important cooling agent of the warm gas and is therefore a very important probe for studying the physical states of the interstellar clouds and the UV fields.

Recent observations have shown that the [C II] line is detected everywhere in the Galactic plane (Shibai et al. 1991; Nakagawa et al. 1992) and at high Galactic latitudes (Bock et al. 1993b). The origin of this diffuse [C II] emission is still uncertain. The [O I] line intensity simultaneously observed with the [C II] line will make it clear whether the [C II] line comes from the diffuse photodissociation regions or the extended H II regions, where there is no neutral oxygen. In addition to the above, the [O I] line has been believed to be emitted from a interstellar gas heated by a shock wave (Holenbach & McKee 1989). The [O I] channel of the FILM will also trace the shocked regions around supernova remnants and in star forming regions.

4.3. *Stars*

Although the IRTS mission is optimized for observations of extended sources, it will also observe many point sources as well, such as late-type stars, stars with mass losses, planetary nebulae, and so forth. The NIRS and the MIRS can together cover the wavelengths from 1.4 to 11.7 μm, where important molecular bands, such as water vapor, ice, CO, and silicate are included. In addition, the sensitivity of the MIRS is a factor of 5 higher than the similar instrument, the Low Resolution Spectrometer (LRS), in the *IRAS* mission, over their overlapping wavelength ranges because of the advances in detector technology. The IRTS is therefore an ideal tool for a systematic study of the structure, atmosphere, and evolution of late-type stars and stars in the late stages of evolution.

4.4. *Extragalactic Background Radiation*

As shown in Figure 8, the brightnesses of the known extended sources are weak in the 3–4 μm and 300–500 μm regions, providing windows through which to search for extragalactic light. It has been theoretically predicted that there is background radiation, other than the famous cosmic microwave background light, that is due to integrated light from all galaxies on the line of sight out to the distance of galactic formation. The large amount of UV and visible radiation emitted when the galaxies were formed will be redshifted to the near-IR wavelength range and may be detected. The extragalactic radiation converted to far-IR light by any dust in the galaxies should be observable in the submillimeter region. Some attempts to measure this background light have been made using sounding rockets (Noda et al. 1992) and the DIRBE experiment of the *COBE* has made an extensive search (Hauser et al. 1991), but definite results have not been obtained yet. This situation exists because observation requires an absolute measurement of sky brightness, and the separation of the isotropic background from foreground emission is a very difficult matter. A systematic search, independent of past observations, is therefore absolutely necessary. The NIRS, which covers the near-IR window, is able to detect stars brighter than 8 mag at 2 μm. We can reduce the integrated light from stars in the Galaxy, one of the sources of foreground radiation, by removing the contribution of those stars from the measured brightness. The observation of interplanetary dust emission by the MIRS is also very important for the separation of foreground radiation. The FIRP will measure the diffuse background in the deep submillimeter window near 400 μm with greater angular resolution than FIRAS, which will assist in the identification and subtraction of local sources of emission.

The observations of interstellar dust emission by the FIRP will also play an important role in the search for the anisotropy of the cosmic microwave background, the seeds of the observed structure in the present-day universe. Several experiments to measure the anisotropy with angular scales smaller than those found by the *COBE* experiment (Smoot et al. 1992) have been designed and are now operating in the millimeter wavelength range (Fischer et al. 1992). Confusion created by interstellar dust emission will ultimately limit the sensitivity of the cosmic background anisotropy at wavelengths below 3 mm. Observations by the FIRP in the submillimeter region will improve the precision with which millimeter wavelength interstellar dust emission can be modeled and subtracted from cosmic microwave background anisotropy measurements.

5. CONCLUSIONS

The IRTS is the first ISAS mission for infrared astronomy. It was initially planned as a step toward regular infrared astronomy space missions of ISAS in the future. The IRTS has already contributed to advances in space cryogenics and infrared-detector technology in Japan. All four FPIs have been installed in the flight-model cryostat, and their performance has been confirmed. The IRTS will make valuable contributions to a wide range of astrophysical problems.

We thank K. Kuriki, the project manager of the *SFU*, M. Natori of ISAS, and other *SFU-1* team members for their kind support of the integration of the IRTS into the *SFU-1*.

Many people have contributed to the IRTS project. We especially thank T. Kono of Tokyo Metropolitan Institute of

Technology for supporting the testing of the telescope system, M. Narita of ISAS for managing testing at ISAS, and N. Hiromoto of the Communication Research Laboratory for preparing the detectors for the FILM.

We would also like to acknowledge corporate contributions to the IRTS project under contract to the ISAS. System integration was performed by the NEC Corporation. The cryostat was built by Sumitomo Heavy Industries. Nikon prepared the telescope and some mirrors for the FPIs. The mirror supports of the telescope system and the mechanical structure of NIRS, MIRS, and FILM were built by Mitaka Koki Company. The detector system of the NIRS was developed by Hamamatsu Photonics K.K. (HPK) in collaboration with Nagoya University. HPK also provided the signal-processing electronics for the FPIs. The fabrication of two of the four FPIs, the MIRs, and the FIRP, have been supported financially by the NASA grants program. T. Y. was supported by the Konica-Tachibana foundation during his work on IRTS.

REFERENCES

Bock, J., & Lange, A. E. 1994, in preparation
Bock, J., Lange, A. E., Matsuhara, H., Matsumoto, T., Onaka, T., & Sato, S. 1994, Appl. Opt., in press
Bock, J., et al. 1993, ApJ, 410, L115
Boulanger, F., Baud, B., & van Albada, G. D. 1985, A&A, 144, L9
Duband, L., Hui, L., & Lange, A. E. 1990, Cryogenics, 30, 263
Fischer, M. L., et al. 1992, ApJ, 388, 242
Hauser, M. G., Kelsall, T., Moseley, S. H., Silverberg, R. F., Murdock, T., Toller, G., Spiesman, W., & Weiland, J. 1991, in After the First Three Minutes, ed. S. S. Holt, C. L. Bennett, & V. Trimple (AIP Conf. Proc. 222) (New York: AIP) 161
Hollenbach, D., & McKee, C. 1989, ApJ, 334, 771
Lange, A. E., Freund, M. M., Sato, S., Hirao, T., Matsumoto, T., & Watabe, T. 1994, ApJ, 428, 384
Mather, J. C. 1982, Opt. Engineering, 21, 769
Murakami, M., et al. 1990, in Advanced Cryogenic Engineering, vol. 35, ed. R. W. Fast (New York: Plenum), 295
Nakagawa, T., et al. 1992, in Back to the Galaxy, ed. S. S. Holt & F. Verter (AIP Conf. Proc. 278) (New York: AIP), 303
Natori, M., & Kuriki, K. 1991, Space Technol., 11, 159
Neugebauer, G., et al. 1984, ApJ, 278, L1
Noda, M., Christov, V. V., Matsuhara, H., Matsumoto, T., Matsuura, S., Noguchi, K., Sato, S., & Murakami, H. 1992, ApJ, 391, 456
Noda, M., Matsumoto, T., Matsuura, S., Noguchi, K., Tanaka, M., Lim, M. A., & Murakami, H. 1994, ApJ, 428, 363
Onaka, T., Yagi, T., Shibai, H., Murakami, H., Tanabe, T., & Kohno, T. 1994, Appl. Opt., in press
Roellig, T. L., Onaka, T., McMahon, T. J., & Tanabe, T. 1994, ApJ, 428, 370
Sato, S., et al. 1994, in preparation
Shibai, H., et al. 1991, ApJ, 374, 522
Shibai, H., Yui, M., Matsuhara, H., Hiromoto, N., Nakagawa, T., & Okuda, H. 1994, ApJ, 428, 377
Smoot, G. F., et al. 1992, ApJ, 396, L1
Wilbanks, T., Devlin, M., Lange, A. E., Sato, S., Becman, J. W., & Haller, E. E. 1990, IEEE Trans. on Nucl. Sci., 37, 566
Winston, R. 1970, J. Opt. Soc. Am., 60, 245
Wright, E. L., et al. 1991, ApJ, 381, 200